Biochem. J. (2013) **451**, 81–90 (Printed in Great Britain) doi:10.1042/BJ20121623

AdE-1, a new inotropic Na^+ channel toxin from *Aiptasia diaphana*, is similar to, yet distinct from, known anemone Na^+ channel toxins

Nir NESHER*†[1], Eli SHAPIRA†, Daniel SHER*‡, Yehu MORAN§, Liora TSVEYER‖, Ana Luiza TURCHETTI-MAIA¶**, Michal HOROWITZ††, Binyamin HOCHNER†** and Eliahu ZLOTKIN*[2]

*Department of Cell and Animal Biology, Institute of Life Sciences, The Hebrew University of Jerusalem, Jerusalem, Israel, †Smith Center for Psychobiology, Institute of Life Sciences, The Hebrew University of Jerusalem, Jerusalem, Israel, ‡Department of Marine Biology, Leon H. Charney School of Marine Sciences, University of Haifa, Haifa, Israel, §Department for Molecular Evolution and Development, Faculty of Life Sciences, University of Vienna, Vienna, Austria, ‖Alomone Labs, Jerusalem, Israel, ¶The Edmond and Lily Safra Center for Brain Sciences, The Hebrew University of Jerusalem, Jerusalem, Israel, **Department of Neurobiology, Institute of Life Sciences, The Hebrew University of Jerusalem, Jerusalem, Israel, and ††Laboratory of Environmental Physiology, Faculty of Dental Medicine, The Hebrew University of Jerusalem, Jerusalem, Israel

Heart failure is one of the most prevalent causes of death in the western world. Sea anemone contains a myriad of short peptide neurotoxins affecting many pharmacological targets, several of which possess cardiotonic activity. In the present study we describe the isolation and characterization of AdE-1 (ion channel modifier), a novel cardiotonic peptide from the sea anemone *Aiptasia diaphana*, which differs from other cnidarian toxins. Although AdE-1 has the same cysteine residue arrangement as sea anemone type 1 and 2 Na^+ channel toxins, its sequence contains many substitutions in conserved and essential sites and its overall homology to other toxins identified to date is low (<36 %). Physiologically, AdE-1 increases the amplitude of cardiomyocyte contraction and slows the late phase of the twitch relaxation velocity with no induction of spontaneous twitching. It increases action potential duration of cardiomyocytes with no effect on its threshold and on the cell's resting potential. Similar to other sea anemone Na^+ channel toxins such as Av2 (*Anemonia viridis* toxin II), AdE-1 markedly inhibits Na^+ current inactivation with no significant effect on current activation, suggesting a similar mechanism of action. However, its effects on twitch relaxation velocity, action potential amplitude and on the time to peak suggest that this novel toxin affects cardiomyocyte function via a more complex mechanism. Additionally, Av2's characteristic delayed and early after-depolarizations were not observed. Despite its structural differences, AdE-1 physiologic effectiveness is comparable with Av2 with a similar ED_{50} value to blowfly larvae. This finding raises questions regarding the extent of the universality of structure–function in sea anemone Na^+ channel toxins.

Key words: cardiomyocyte, cardiotonic effect, peptide purification, sea anemone, sequence alignment, sodium channel toxin.

INTRODUCTION

HF (heart failure), defined as the inability of the heart to meet the metabolic demands of the body [1], is an increasing concern worldwide. HF is a deteriorating syndrome characterized by mortality of approximately 50 % of patients within 5 years [2]. Although tremendous progress has been made in the development of drugs that decrease the mechanical load on the myocardium [3], no progress has been made in developing new positive inotropic agents which can improve the symptoms of the disease [4]. Furthermore, the most common positive inotropic drugs used in standard therapy involves risk to the patients owing to their narrow therapeutic window and in turn toxicity [5]. There is an immense need for new active substances for research and drug development.

Sea anemones (Anthozoa, Actinaria) are sessile predators living in marine habitats worldwide. Sea anemones possess an impressive arsenal of bioactive peptides and chemicals used for prey capture and for defence against predators [6]. Among these peptides are pore-forming toxins and cytolysins [7], toxins affecting ion channels as voltage-gated Na^+ channels [8,9] and voltage-gated K^+ channels [8], toxins affecting pain sensing as acid-sensing ion channels and vanilloid receptors [10,11], proteinase inhibitors [12], EGF (epidermal growth factor)-like toxins [13] and cardiotonic peptides. An example of the latter is ApA (Anthopleurin A), from the sea anemone *Anthopleura xanthogrammica*, which produces a strong positive inotropic effect in various animal species with no effect on heart rate, blood pressure or Na^+/K^+-ATPase [14].

The sea anemone *Aiptasia diaphana* (Cnidaria, Anthozoa, Actiniaria, Aiptasiidae) is a small anemone found on immersed objects in the photic zone of the Israeli Mediterranean sea coast. *A. diaphana* obtains at least part of its diet by hunting, utilizing tentacle-derived toxins to paralyse their prey before inserting it into their gastro-vascular cavity. Additional toxins are found in the acontial filaments within the gastrovascular cavity, possibly to enhance prey degradation [15]. Although *A. diaphana*'s prey is usually relatively small, we have observed individuals of approximately 5 cm length and 2 cm crown diameter catching, paralysing and swallowing fish approximately 2 cm long, suggesting this species possesses highly effective neurotoxins. Interestingly, although *A. diaphana* toxins show strong effects on crustaceans, insects and fish, humans are not sensitive to their sting.

Abbreviations used: AdE-1, ion channel modifier; AP, action potential; ApB, anthopleurin-B; APD, AP duration; APD_{50}, APD at half of AP amplitude; Av2, *Anemonia viridis* toxin II; DDW, double distilled water; HF, heart failure; Na_V1, Na^+ channel, voltage-gated; $hNa_V1.5$, human Na_V1 type V; RACE, rapid amplification of cDNA ends; rAdE-1, recombinant AdE-1; TD_{30}, twitch duration at 30 % amplitude; TFA, trifluoroacetic acid; UTR, untranslated region.

[1] To whom correspondence should be addressed (email nir.nesher@mail.huji.ac.il).

[2] This work is dedicated to the memory of Professor E. Zlotkin, a true scientist and a mentor.

In light of this background and the multipotent toxins arsenal of sea anemones affecting a large battery of targets, the goal of the present study was to identify and purify cardioactive peptides in order to contribute to the fields of heart physiology, pathology and drug development research.

EXPERIMENTAL

Crude extractions

A. diaphana specimens were collected along the Israeli Mediterranean coast from spring to summer. The animals were first stressed by immersion in DDW (double distilled water), which induced nematocysts discharge, and then were manually homogenized in this water with a glass homogenizer. The extract was centrifuged at 15000 ***g*** for 15 min at 4 °C and the supernatant collected and filtered (0.45 μm cellulose acetate filters). The crude extract was desalted by passing it through a gravity flow Sephadex G10 (Pharmacia) 90 cm×3 cm column at a flow rate of 1 ml/min, freeze-dried to powder and kept at − 20 °C.

Isolation and characterization of substance AdE-1 (ion channel modifier)

The desalted crude extract was suspended in DDW and fractionated by size-exclusion using a Sephadex G75 (Pharmacia) 90 cm×1 cm column on an FPLC system (Biologic HR, Bio-Rad Laboratories) with DDW as an elution buffer and a flow rate of 1 ml/min. The column's effluent was monitored by absorbance at 280 nm. We proceeded with three separate reversed-phase fractionations on three different columns using a HPLC system (Jasco: LG-1580-04, PU-1580 and MD-1510). The column's effluent was monitored by absorbance at 215 nm and 280 nm. Columns were eluted with 0.1 % TFA (trifluoroacetic acid) in DDW (solvent A) and acetonitrile containing 0.1 % TFA (solvent B). The separations were performed by steps of increased linear gradients of solvent B. The first fractionation was performed on an Atlantis dC18, 5 μm 4.6×250 mm column (Waters) with a flow rate of 0.5 ml/min according to the protocol: 10 min of 3 % solution B followed by 42 min of linear gradient from 3 % to 43 % and then from 43 % to 100 % of solution B in 8 min. The second fractionation was performed on a Lichrocart 100RP-18, 5 μm 4.0 mm×250 mm column (Merck) with flow rate of 1 ml/min in a protocol of 5 min of 3 % solution B, followed by 50 min of linear gradient from 3 % to 45 % of solution B. The third and final fractionation was performed on an analytical C18, 5 μm 4.6 mm×250 mm column (Vydac) with flow rate of 1 ml/min and the following protocol: 5 min of 3 % solution B followed by 10 min of linear gradient from 3 % to 20 % of solution B, then 10 min of 20 % solution B, followed by 30 min of linear gradient from 20 % to 45 % of solution B.

MS

The molecular mass of substance AdE-1 was determined using a Voyager DE-Pro MALDI–TOF (matrix-assisted laser-desorption ionization–time-of-flight) mass spectrometer (Applied Biosystems) with α-cyano-4 -hydroxycinnamic acid as the matrix.

Determination of AdE-1 concentration

AdE-1 concentrations were determined by measuring the absorbance at 228 nm and 234 nm. The concentration was then calculated using the equation (228 nm value − 234 nm value)×K, where $K = 65.5$ and is the slope constant determined by the linear equilibration curve with known increasing concentrations of Av2 (*Anemonia viridis* toxin II).

AdE-1 cloning, cDNA and genomic DNA sequence identification

The N-terminal 30 amino acids of AdE-1 were sequenced by N-terminus sequence analysis (Edman degradation process) on a Procise 490-1 Sequencer (Applied Biosystems) at the Protein Analysis Unit at the Weizmann Institute for Science, Rehovot, Israel. Total RNA was extracted from whole *A. diaphana* with Tri-Reagent (Sigma) according to the manufacturer's instructions. The isolated RNA was used for cDNA synthesis and cloning using FirstChoice RLM-RACE kit (Ambion). The 5′-terminus of *AdE-1* cDNA sequence was cloned using outer (5′-GAYAARAAYWSIGAYGARTGYAA-3′) and nested (5′-ATGAAYGGNAAYTGYGGNGAYGG-3′) degenerate primers designed according to the N-terminal sequence determined by the Edman degradation process, and the outer and the nested primers of the kit. The product of the nested PCR was ligated into pGEM-T-Easy vector (Promega) and sequenced. To identify the whole precursor sequence, 5′-RACE (rapid amplification of cDNA ends) was performed by two subsequent PCRs, using sequence-specific outer (5′-TGCATTACTAAACTCTTTGACAACAA-3′) and nested (5′-CTTTGACAACAATTGAAAATTGC-3′) primers, which were designed based on the 3′-RACE results and the outer and nested 3′-RACE primers of the kit. Finally, to verify the results, *AdE-1* cDNA was amplified using gene-specific primers designed from *AdE-1* cDNA 5′- (5′-TCGAAGAAAAGTCGGGACTAA-3′) and 3′- (5′-ATGCGCGGCCGCTTGACAACAATTGAAAATTGCAT-3′) ends and sequenced. PCR was carried out under the following conditions: 3 min at 94 °C, 35 cycles of (94 °C for 30 s, 60 °C for 30 s and 72 °C for 30 s) and 7 min at 72 °C. Genomic DNA was extracted from *A. diaphana* with TRI Reagent (Sigma) according to the manufacturer's instructions. The isolated DNA was used for *AdE-1* gene sequence amplification by PCR using gene-specific primers designed from *AdE-1* cDNA 5′- (5′-TCGAAGAAAAGTCGGGACTAA-3′) and 3′- (5′-ATGCGCGGCCGCTTGACAACAATTGAAAATTGCAT-3′) ends and sequenced. All sequencing procedures were carried out at the Genomic Center of the Life Sciences Institute at The Hebrew University of Jerusalem, Jerusalem, Israel.

Expression of rAdE-1 (recombinant AdE-1)

The mature AdE-1 was expressed as a fusion protein, with a His_6 tag and the fluorophore mCherry fused to AdE-1's C-terminus (AdE-1–mCherry–His). This was constructed in the pET-32a vector (Novagen). Expression was performed in the Origami *Escherichia coli* strain (Novagen), grown to an attenuance of $D = 0.6$, induced by IPTG (isopropyl β-D-thiogalactopyranoside; 0.2 mM) and incubated overnight at 20 °C. The cells were lysed by sonication (cycles of 1 s on then 1 s off for 10 min at 40 % acoustic power; Sonics Vibra Cell, VCX750, 750 W, 20 kHz) in Tris/HCl buffer (pH 7.1), centrifuged at 12000 ***g*** for 20 min at 4 °C, mixed with equilibrated nickel–agarose resin (Adar Biotech) for 60 min at 4 °C, washed four times with Tris/HCl buffer and eluted with 250 mM imidazole in Tris/HCl buffer. The imidazole was removed from the elution buffer using 10KD spin concentration tubes (Millipore) to provide the pure rAdE-1.

Sequence analysis and alignments

The various DNA sequences encoding AdE-1 were aligned using the global alignment of two nucleotide sequences version 2.2u, on

the ExPASy Server of the Swiss Institute of Bioinformatics [16]. The cDNA translation to amino acid sequence, the molecular mass and pI estimation were performed using the protein identification and analysis tools on the ExPASy Server [17]. Multiple alignments were performed using ClustalW 2.0.12 at EMBL EBI website [18,19]. Phylogenetic analyses were conducted in MEGA4 [20]. Evolutionary history was inferred using the Neighbor-Joining method [21], with the bootstrap consensus tree inferred from 2000 replicates [22]. Branches corresponding to partitions reproduced in less than 50 % bootstrap replicates were collapsed. All positions containing gaps and missing data were eliminated from the dataset (complete deletion option). The toxins and organisms shown in Figure 5 are as follows: ApB (anthopleurin-B) are from *Anthopleura xanthogrammica*; AM-3 from *Antheopsis maculata;* Av1 (*A. viridis* toxin I) and Av2 from *A. viridis*; AFT-1 (*Anthopleura fuscoviridis* neurotoxin-1) from *A. fuscoviridis*; Halcurin from *Halcurias* sp.; RTX-1 from *Radianthus* (*Heteractis*) *macrodactylus*; Rp-2 from *Radianthus (Heteractis) paumotensis*; Sh-1 (*Stichodactyla helianthus* neurotoxin-1) from *S. helianthus*; gigantoxin-2 and -3 from *Stichodactyla gigantea*; HK-7 from *Anthopleura sp.*; Bg-2 from *Bunodosoma granulifera;* APE-1.1 from *Anthopleura elegantissima*; AETX-1 from *Anemonia erythraea*; Bc-3 from *Bunodosoma caissarum;* CgNa from *Condylactis gigantea*; CGX (cangitoxin) from *Bunodosoma cangicum;* and AdE-1 from *A. diaphana*.

Structural modelling of AdE-1

The structural model of AdE-1 was constructed using the SWISS-MODEL program [23] based on the NMR structure of the type 1 sea anemone toxin CgNa (PDB code 2H9X). The models of AdE-1, ApB (PDB code 1APF; [24]) and Av2 [25] were visualized using DeepView/Swiss PdbViewer version 3.7 and rendered using PovRay version 3.6.2 (Persistance of Vision RayTracer).

Haemolysis assays

Haemolysis assays were performed on human erythrocytes following the method of Primor and Zlotkin [26]. Briefly, human erythrocytes were washed with PBS [120 mM NaCl and 10 mM buffer phosphate (pH 7.4)]. Following washing the erythrocytes were resuspended in PBS to a concentration of 20 % (v/v). The erythrocyte solution was mixed with the inspected fraction suspended in PBS in a ratio of 20:80 (final erythrocyte concentration of 4 %). The tubes were incubated for 1 h at 37 °C. As a positive control the inspected material and the PBS were replaced with DDW (causing the cells to rupture owing to osmotic pressure) and as a negative control the inspected material was replaced with PBS. After the incubation, PBS was added to a volume of 200 % of the reaction volume and then the tube was gently shaken and centrifuged for 3 min at 2000 ***g*** at room temperature (~25 °C). The supernatant was collected and the absorbance was detected at a wavelength of 540 nm. The results were normalized to the absorbance value of the positive control (referred to as 100 % haemolysis).

Paralysis assays

Paralysis assays were performed on 4-day-old (60–80 mg body mass) larvae of the blowfly *Sarcophaga falculata*. Five toxin concentrations were injected intersegmentally at the rear part of the body. A positive result was scored when a characteristic paralysis (immediate spasm which progressed to body contraction and paralysis) was obtained and lasted at least 10 min. The ED_{50} values were calculated as described previously by Zlotkin et al. [27].

Isolating and maintaining cardiomyocytes from the adult rat

The use of animals in the experiments conformed to the protocols and ethics set by the Committee of The Hebrew University of Jerusalem for Animal Care and Use under License number NS-02-13. We used a slightly modified protocol of adult rat cardiomyocyte isolation, kindly provided by Professor Philip Palade (Department of Pharmacology and Toxicology, University of Arkansas for Medical Sciences, Little Rock, AR, U.S.A.). At 30 min prior to anaesthesia, 175–250 g adult male Sprague–Dawley rats were injected intraperitoneally with heparin [0.5 ml 1000 USP (United States Pharmacopeia) units/ml]. The rats were anaesthetized by intraperitoneal injection of ketamine/xylazine (8.5 mg/100 g body mass of ketamine in 0.5 % xylazine) and their heart was removed and attached to a cannula connected to a series of condensers containing various solutions (see details below) warmed to 37 °C and oxygenated with a mixture of 95 % oxygen and 5 % CO_2. Hearts were then subjected to reverse Langendorff perfusion through the aorta at a constant rate of 10 ml/min with modified Tyrode's solution [120 mM NaCl, 15 mM $NaHCO_3$, 5.4 mM KCl, 5 mM Hepes Na^+ salt, 0.25 mM NaH_2PO_4 and 0.5 mM $MgCl_2$ (pH 7.4)] containing 1 mM Ca^{2+} ($CaCl_2$) for 2–3 min and then for 5 min with Ca^{2+}-free modified tyrode solution. Next, the hearts were perfused for 10 min with 100 ml of modified Tyrode's solution containing 0.25 mM $CaCl_2$, 17 mg of collagenase type II (Worthington) and 0.8 mg of protease type XIV (Sigma). The hearts were then removed from the cannula and the ventricles were removed and soaked in 3 ml of KB solution [70 mM KOH, 50 mM glutamic acid, 40 mM KCl, 20 mM taurine, 20 mM KH_2PO_4, 10 mM glucose, 10 mM Hepes, 0.5 mM EGTA and 3 mM $MgCl_2$, (pH 7.4) with KOH], cut into small pieces and triturated in a larger volume of KB solution with a wide-bore plastic pipette. The resulting soup-like solution was filtered through silk and the cells were stored in the KB solution at 4–8 °C. The cells were used for experiments for up to 24 h. Only intact rod-shaped cells, with clear striation, no micro-blebs and which showed no spontaneous contractions, were used for the various experiments.

Measurement of cardiomyocyte contraction

The shortening of rat ventricular cardiomyocytes was measured using an edge-detection video system (Crescent Electronics) as described previously [28]. Cells were viewed with a Nikon Diaphot 200 inverted microscope. Felix software program (PTI) was used for histogram visualization and to analyse and store data. Experiments were performed at room temperature. Cells were placed in a chamber and perfused with Krebs solution [1.2 mM $MgSO_4$, 25 mM $NaHCO_3$, 11 mM glucose, 4.7 mM KCl, 1.25 mM $CaCl_2$, 1.2 mM KH_2PO_4 and 118 mM NaCl (pH adjusted to 7.4 with NaOH)], oxygenated with 95 % O_2 and 5 % CO_2. The cardiomyocytes were field-stimulated (0.5 Hz, square waves), and the amount of shortening (fraction of total length, i.e. the amplitudes of systolic motion) was measured.

Measurements of cardiomyocyte AP (action potential)

The APs of rat ventricular cardiomyocytes were measured during continuous superfusion, using a homemade system for rapid solution changes allowing application of perfusion solution or drugs in the close vicinity of the cells. All measurements were performed at room temperature using a whole-cell patch-clamp single-electrode current-clamp technique in a bridge mode using

an Axoclamp 2B (Axon Instruments) amplifier. Pipettes were pulled on a pp-830 puller (Narishige) with a two-step procedure. The resistances of the pipettes were 2–4 MΩ. After establishing the whole-cell configuration, the AP was elicited by current injection (duration 2 ms, amplitude 3–5 nA, 0.2 Hz) from a holding potential of −90 mV. The superfusion solution contained 150 mM NaCl, 5.4 mM KCl, 10 mM Hepes, 2 mM $MgCl_2$, 2 mM $CaCl_2$ and 20 mM glucose (pH 7.4). The pipette solution contained 40 mM KCl, 8 mM NaCl, 100 mM D,L-K-aspartate, 5 mM Mg-ATP, 5 mM EGTA, 2 mM $CaCl_2$, 10 mM Hepes and 0.1 mM Tris-GTP (pH 7.4). A software program written in Labview was used to store and analyse the data digitally. Data were sampled at 20 kHz, processed using Excel software and are shown as means ± S.E.M. Statistical differences were evaluated by using the Excel software function of two-tailed paired Student's *t* test. $P < 0.05$ was considered statistically significant.

Recording of Na^+ current from $hNa_V1.5$ [human Na_V1 (Na^+ channel, voltage-gated), type V] channels expressed in *Xenopus laevis* oocytes

X. laevis oocytes were obtained surgically from adult *X. laevis* females anaesthetized with MS-222 (Sigma–Aldrich), as described previously [29]. The oocytes were treated with collagenase Type II (500 units/ml, Sigma–Aldrich) in a Ca^{2+}-free ND-96 solution [96 mM NaCl, 2 mM KCl, 1 mM $MgCl_2$ and 5 mM Hepes (pH 7.4)] with gentle shaking at 22 °C for 1 h. The oocytes were then rinsed with ND-96 solution containing 1.8 mM $CaCl_2$ to remove collagenase and debris. Stage V–VI oocytes were selected and incubated for 24 h at 18 °C in enriched ND-96 solution, containing 1.8 mM $CaCl_2$ and supplemented with 2.5 mM sodium pyruvate (Biological Industries) and 10 units/ml penicillin and 10 μg/ml streptomycin (Biological Industries). cRNA coding for $hNa_V1.5$ was prepared using a T7 *in vitro* transcription kit (Epicentre Biotechnologies) from $hNa_v1.5$ cDNA in the PGEM-3 plasmid, linearized with HindIII (New England Biolabs). cRNA product was monitored by gel electrophoresis and absorbance measurements. Using a 10 μl microdispenser (Drummond Digital 510) *X. laevis* oocytes were microinjected with the $hNa_V1.5$ cRNA (50 ng/oocyte, final volume of 50 nl/oocyte) and incubated at 18 °C in enriched ND-96 solution for 4–6 days prior to the electrophysiological measurements in order to allow optimal expression of the channel protein [30]. Whole-cell membrane currents were recorded by applying two-electrode voltage clamp using a GeneClamp 500B amplifier and DigiData 1322A digitizer (Axon Instruments) in ND-96 bath solution supplemented with 1.8 mM $CaCl_2$. A voltage ramp of 40 ms from a holding potential of −100 mV up to +60 mV was applied every 10 s. Current traces were leak-subtracted on-line using Clampex 8.1 software (Axon Instruments). AdE-1 in bath solution was applied via perfusion for 100 s.

RESULTS AND DISCUSSION

Isolation of AdE-1, a cardiotonic peptide from *A. diaphana*

The crude water extract of *A. diaphana*, like that of many other cnidarians, revealed several different biological activities. It has a haemolytic effect ($EC_{50} \sim 2$ μg/ml) and causes immediate paralysis and body contraction when injected into blowfly larvae ($ED_{50} \sim 0.75$ ng/mg of body mass; Supplementary Figure S1A at http://www.biochemj.org/bj/451/bj4510081add.htm). The crude extract is cardiotonic, increasing the amplitude of cardiomyocyte contraction and induces spontaneous twitching (Supplementary Figure S1B). It affects cardiomyocyte excitation by increasing the APD (AP duration), raising the AP peak amplitude and increasing its rising phase slope (Supplementary Figures S1C and S1D).

Next, we isolated a cardioactive peptide from the crude homogenate using a series of chromatographic steps. The desalted crude extract was separated according to molecular size using a Sephadex G75 column with DDW as the elution buffer. The low molecular mass fraction enhanced cardiomyocyte contraction and was subjected to three subsequent rounds of HPLC reversed-phase fractionation (Figure 1). By this separation process we isolated a cardioactive peptide with no haemolytic activity on human erythrocytes, and with no effect on the shape, colour and configuration of cardiomyocytes (visual inspection). It was also paralytic to the blowfly larvae *S. falculata*, causing an immediate spasm that progressed to body contraction and paralysis with an ED_{50} of 16.91 ± 5.78 ng/g of body mass. This ED_{50} value is very similar to that of Av2 (18.25 ng/g of body mass) [25], one of the first sea anemone Na^+ channel neurotoxins to be isolated and studied in detail [31]. The molecular mass of the peptide, which we named AdE-1, was determined by mass spectrometry to be 4907 Da (Figure 1E) and its sequence was identified (GenPept accession number ACQ83467, described in detail later).

AdE-1 has multiple effects on isolated cardiomyocytes

Similar to the crude water extract, AdE-1 increased the amplitude of cardiomyocyte contractions. This effect was accompanied by a clear slowing of the late phase of the twitch relaxation and a prolongation of the total twitch time (Figure 2). For example, 10 ng/ml of AdE-1 increased the twitch amplitude approximately by 2-fold (106 ± 6.6 %) and the TD_{30} (twitch duration at 30 % amplitude) by 50.46 ± 7.77 %, $P < 0.01$ (Figures 2C and 2D). The twitch prolongation effect is due mainly to the increased relaxation time as no change in the twitch's contraction phase kinetics was observed (Figure 2B). Importantly, we did not observe any spontaneous twitches as those induced by the crude extract.

Contraction performances are tightly coupled to excitation pattern in cardiomyocytes [32]. We therefore investigated the effects of AdE-1 on the AP of isolated cardiomyocytes. The first noticeable effect was a significant concentration dependent increase in the APD (Figures 3A and 3F). The minimal concentration of toxin necessary for APD_{50} (APD at half of AP amplitude) prolongation was approximately 0.1 ng/ml and the EC_{50} value was 63.7 ± 13.9 ng/ml (Figure 3F). In addition, AdE-1 decreased the AP's time to peak and has biphasic effects on its amplitude; at low concentrations (<3.5 ng/ml) we observed an increase in the AP amplitude, but at concentrations above 3.5 ng/ml, both the amplitude and time to peak showed concentration-dependent decreases and were significantly lower than the control (Figures 3C and 3E). For example, AdE-1 at a concentration of 135 ng/ml decreased significantly the AP amplitude from 137.28 ± 1.43 mV to 126 ± 0.64 mV ($n = 5$, $P \leqslant 0.0037$) and the time to peak from 2.61 ± 0.17 ms to 2.175 ± 0.13 ms ($n = 5$, $P \leqslant 0.038$). These effects were not observed after Av2 application (tested at a concentration range of 0.1 ng/ml–10 μg/ml, Figure 3D). We did not observe significant effects on AP threshold, AP rising phase slope and the cells' resting potential. Interestingly, no early after-depolarizations or delayed after-depolarizations, characteristic effects of Av2, were observed (for the Av2 early and delayed after-depolarizations see Figure 3B). All of AdE-1's effects were highly reversible (following washout more than 90 % recovery was achieved in less than 30 s).

The prolongation of the AP by AdE-1 is likely to be caused by the well-known effect of sea anemone toxins on Na^+ current by which the toxins interact with the Na^+ channels site-3 and inhibit the transition of the channels to inactivation state.

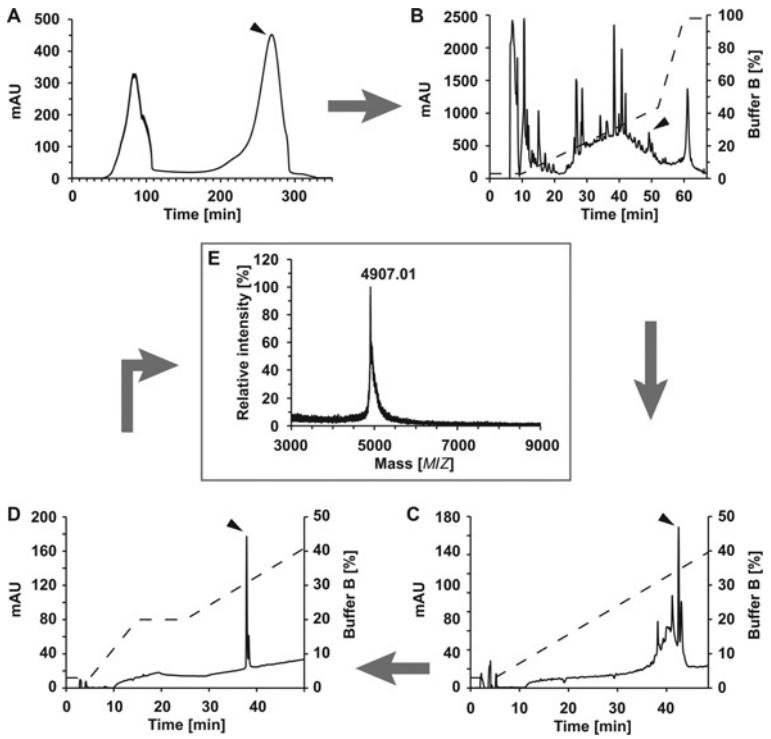

Figure 1 The isolation and purification process of AdE-1

(**A**) Molecular exclusion of *A. diaphana* crude extract on Sephadex G75 column with DDW as the elution buffer. (**B**) Peak 2 was subjected to fractionation on a reversed-phase HPLC Atlantis dC_{18}, 5 μm column. (**C**) The resultant peak was subjected to further purification on a Lichrocart 100RP-18, 5 μm column. (**D**) The final purification was carried out on a C_{18}, 5 μm 4.6 mm$\times$250 mm column (Vydac). The elution buffers for the reverse-phase HPLC fractionations were: A, DDW with 0.1 % TFA and B, acetonitrile with 0.1 % TFA. The broken line represent the percentage of buffer B in time. (**E**) MS showed that the molecular mass of the resultant peak was 4907 Da. Arrow heads indicate the selected peak and grey arrows indicate the order of purification. mAU, milli-absorbance units.

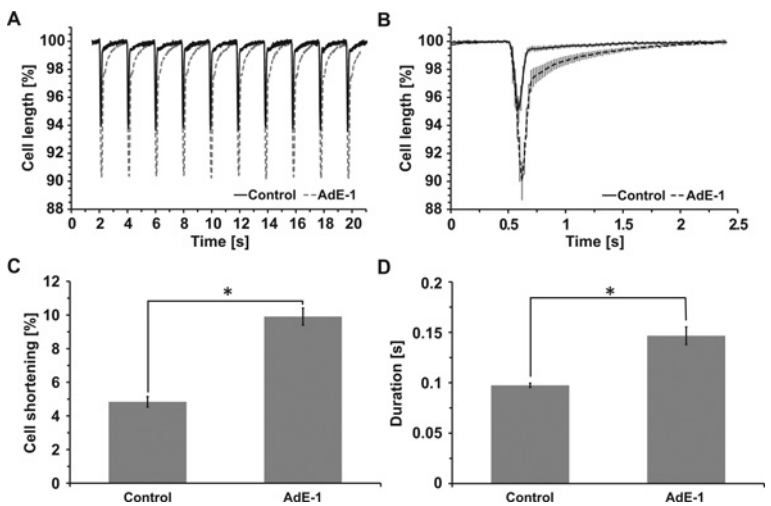

Figure 2 Effects of AdE-1 on the contractions of isolated cardiomyocytes

AdE-1 (10 ng/ml) increased the contraction amplitude, slowed the relaxation speed and prolonged the cells' TD_{30} value. (**A**) Example of myocyte contraction before and after the application of AdE-1. (**B**) Outcome of 100 twitches before and after the application of AdE-1. AdE-1 increases the twitch amplitude and duration with no substantial effect on the contraction phase dynamics. The twitch prolongation is mainly due to the velocity deceleration of the late-relaxation phase. Results are means $\pm$ S.E.M, $n = 10$ cells. AdE-1 effects on twitch amplitude (**C**) and AdE-1 effects on the TD_{30} value (**D**). Results are means $\pm$ S.E.M. *$P < 0.01$ determined by two-tailed paired Student's *t* test. Contractions were evoked by external stimulation of 0.5 Hz.

Indeed, similar to the effect of Av2, AdE-1 (20 ng/ml) markedly inhibits the inactivation of Na^+ current from $hNa_V1.5$ channels subtype, which were expressed in *Xenopus laevis* oocytes, with no significant effect on current peak amplitude, threshold for activation, rising phase slope and time to peak (Figure 4). $Na_V1.5$ is the main Na^+ channel subtype in mammalian ventricular cardiomyocytes [33]. These results strongly suggest that the main effect of AdE-1 on cardiomyocyte excitation, the same as Av2 and other type 1–2 sea anemone toxins, is through direct interaction of the toxin with Na^+ channels receptor site-3.

The increase in Na^+ current by sea anemone Na^+ channel toxins led to a rise in Ca^{2+} influx through both the voltage-dependent

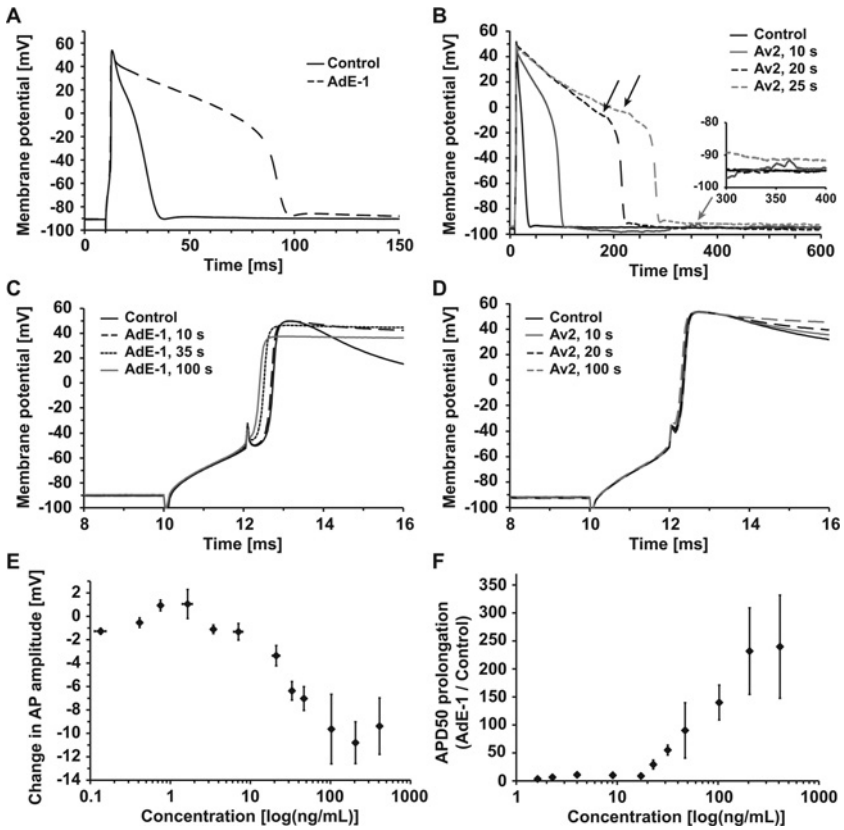

Figure 3 Effects of AdE-1 and Av2 on the AP of isolated cardiomyocytes

(**A**) AdE-1 (10 ng/ml) prolonged the AP and slightly decreased the AP peak amplitude with no induction of early after-depolarization or delayed after-depolarization. (**B**) Av2 (10 ng/ml) prolonged the APD and induced early and delayed after-depolarization (black and grey arrows respectively). The effect of delayed after-depolarization is enlarged in the inset. (**C**) High concentrations of AdE-1 (135 ng/ml) decreased the time to peak and the AP amplitude. These effects distinguish AdE-1 effects from the effects of Av2 and other sea anemone Na^+ channel toxins as demonstrate in (**D**). (**D**) Av2 (100 ng/ml) prolonged APD with no significant effect on the time to peak and on AP amplitude. (**E**) AdE-1 affects AP amplitude in a biphasic manner. At low concentrations the AP amplitude was increased, but it decreased in a concentration-dependent manner at concentrations above 3.5 ng/ml. (**F**) AdE-1 prolonged the APD in a concentration-dependent manner. The EC_{50} value is 63.7 $\pm$ 13.9 ng/ml. Each point in (**E**) and (**F**) is the mean $\pm$ S.E.M of data from three to six cells. The *x*-axes in (**E**) and (**F**) are a logarithmic scale.

Ca^{2+} channels and the Na^+/Ca^{2+} exchanger. This leads to a greater Ca^{2+} release from intracellular stores, and a consequent increase in cytosolic Ca^{2+} concentration that enhances muscle contraction [9,34]. As mentioned above, AdE-1 probably affects cardiomyocytes through a similar mechanism. However, the AdE-1-induced acceleration of AP rising phase, shortening of AP time to peak and decrease in AP peak amplitude (Figure 3), all suggest that there are subtle differences in the molecular mode of action. In addition, the slowing of the late twitch relaxation-phase rate (Figure 2) is an effect that is not described for the known sea anemone Na^+ channel toxins, suggesting additional or different mechanisms of the effect of AdE-1 action.

Finally, under the conditions tested in the present study, AdE-1 did not induce early after-depolarization nor delayed after-depolarization, which are both typical effects of Av2 on cardiomyocyte AP (compare Figures 3A and 3B) [35,36]. Elucidating the reason why AdE-1, unlike Av2, does not cause these effects may contribute to the design of better therapies for heart failure.

Sequencing and cloning of AdE-1

To obtain the full sequence of AdE-1, we sequenced the N-terminal 30 amino acids by Edman degradation, and used this sequence to design degenerated primers for PCR. The resulting cDNA sequence encodes an AdE-1 precursor (GenBank® accession number FJ418889) consisting of 90 amino acids, of which 44 amino acids are the mature toxin and the other 46 amino acids are the leader peptide (Supplementary Figure S2 http://www.biochemj.org/bj/451/bj4510081add.htm). The latter is probably composed of a pro-peptide and a signal peptide as it ends with a pair of basic residues (Lys–Arg), which appears in numerous cnidarian secreted peptides and is likely to be recognized by a protease during toxin maturation [37]. The mature peptide is predicted to be slightly basic (theoretical pI = 7.77), and the calculated molecular mass agrees with the experimentally determined one (4907 Da). Thus mature AdE-1 does not undergo post-translational modifications besides the formation of three disulfide bridges, which probably form a scaffold similar to that of known sea anemone type 1 and 2 Na^+ channel neurotoxins (Figures 5A and 5C). The cDNA also contained 5′- and 3′-UTRs (untranslated regions; 69 bp and 39 bp respectively).

To verify that the cloned sequence represents AdE-1 and that the physiological activity is not due to undetected impurities, we expressed rAdE-1 fused with mCherry fluorophore and a His-tag fragment at the toxin C-terminus (Ade-1–mCherry–His). rAdE-1 was purified and its activity was tested. rAdE-1 (100 ng/ml) [100 ng/ml of the rAdE-1 (molecular mass $\sim$ 33 kDa) has almost the same molar concentration as 10 ng/ml of the purified AdE-1 (molecular mass $\sim$ 5 kDa), $\sim$ 3 nM and $\sim$ 2 nM respectively] caused *S. falculata* larvae (0.08 g on average) immediate spasm which progressed to body contraction and

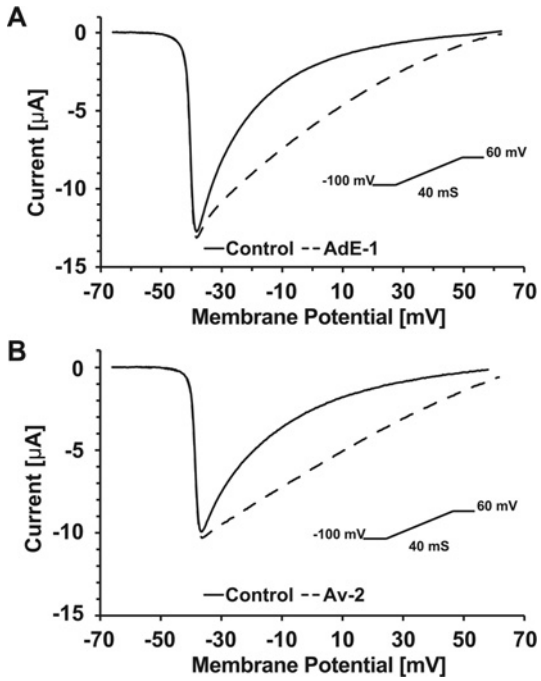

Figure 4 AdE-1, similarly to Av2, inhibits the inactivation of Na^+ current from $hNa_V1.5$ channels expressed in *X. laevis* oocytes

(**A**) AdE-1 (20 ng/ml) inhibited current inactivation. No effects on the current activation voltage, slope of the current rising phase and current time to peak could be seen. The increase in the current amplitude was not significant, $P \leqslant 0.25$. (**B**) Av2 (100 ng/ml) affected the current in a similar phenotype. Current was evoked by a voltage ramp from − 100 mV to 60 mV in 40 ms. Traces were evoked every 200 ms.

paralysis; it prolonged the APD and slightly decreased AP amplitude of isolated cardiomyocytes (Supplementary Figure S3 at http://www.biochemj.org/bj/451/bj4510081add.htm). The effects observed were not owing to the mCherry or His tags or to the buffers used in extraction and purification of the proteins, since two other toxin peptides from the scorpion (GenPept accession number AAV54593) and wasp (GenPept accession number P69392) which affect Na^+ channels, but not the cardiac channel subtype ($Na_V1.5$) [38,39], were expressed with the same system, caused contraction and paralysis to *S. falculata* larvae, but had no effect on cardiomyocyte AP.

The cDNA sequencing was followed by determination of the genomic structure of the locus encoding AdE-1. When primers designed to amplify the full cDNA sequence were used to amplify genomic DNA (see the Experimental section for details), three distinct amplicons were obtained. The largest (1630 bp) encoded a gene composed of three exons and two introns. The first exon included the 5′-UTR, the second encoded a small part of the 5′-UTR and the leader part and the third exon encoded the remainder of the leader and the mature toxin (Figure 6). A similar gene organization has been described for other sea anemone toxins as well as unrelated toxins from other organisms [40].

In addition to this canonical toxin gene, two shorter amplicons, one of 650 bp and the other of 600 bp, were observed. The 650 bp amplicon is almost identical with the full-length gene, with the only difference being a 930 bp deletion in the second intron (Figure 6 and Supplementary Figure S4 at http://www.biochemj.org/bj/451/bj4510081add.htm). The 600 bp amplicon, in contrast, contained only two exons, lacking exon 2, which encodes part of the 5′-UTR and most of the leader sequence. Intriguingly, whereas the coding sequence for the mature peptide of the 600 bp fragment is almost identical with that of the 1630 bp gene, the intron sequence includes indels and is quite different (Figure 6 and Supplementary Figure S5 at http://www.biochemj.org/bj/451/bj4510081add.htm). A similar phenomenon was described for the multiple genomic loci of Av2 in *A. viridis* [41]. When PCR amplification was performed on genomic DNA extracted from single animals ($n = 6$), only one of the short amplicons was observed, whereas the full-length (1630 bp) sequence was always observed. This suggests that the 600 and 650 bp sequences are alleles of the same locus.

Multiple sequence comparison of AdE-1 with various sea anemone type 1 and type 2 Na^+ channel toxins

The highest amino acid sequence identity of AdE-1 to any known toxin is only 36 % shared with AM-3, a toxin from the sea anemone *A. maculata* [42]. However, its primary structure suggests a relationship with the most commonly studied groups of sea anemone toxins, the type 1 and type 2 Na^+ channel neurotoxins. Indeed, multiple sequence alignment of AdE-1 with various type 1 and type 2 Na^+ channel toxins revealed that AdE-1 shares common residues in several conserved sites including Asp^7, Gly^{15}, Gly^{22}, Gly^{34} and Trp^{35} (numbering is as in Figure 5A). Nevertheless, AdE-1's sequence differs in most of its other residues from these groups of toxins including several non-conservative substitutions at highly conserved sites, such as D9N, G10S, P11D, R14N and K50Q (Figure 5A). In model type 1 and type 2 neurotoxins several of these residues are known to be important to the stability, binding or biological activity of these toxins (see below). In addition, the multiple sequence alignment emphasizes that the distribution of acidic, basic, hydrophilic and hydrophobic residues over the toxin sequence differ in AdE-1 sequence compared with other toxins of these groups. The complete absence of a highly hydrophobic region between residues 23 and 27 is prominent. This region is thought to play a pivotal role in folding and toxin structure [25]. These differences are also prominent along the 'Arg^{14} loop' region. In type 1 and 2 sea anemone Na^+ toxins the Arg^{14} loop is the region from sites 8–17 thought to play an important role in the toxin's interactions with the channels [43,44]. Residues in sites 9, 12, 16 and 20, suggested to play an important role in the toxin's bioactivity, and glycine residues in positions 10, 15 and 22 are conserved and seem to occupy key positions for the flexibility of the loop [9,25,43]. The degree of tilting is considered to play an important feature of the loop, and is suggested to be essential for the interaction with the receptor site [25,45]. Mutagenesis of these glycine residues decreased toxin activity [43]. Comparison of the sequence of AdE-1 with other sea anemone Na^+ toxins reveals that one of these glycine residues (Gly^{10} in Figure 5A) is replaced by serine and most of the common residues of the Arg^{14} loop are different in AdE-1, including residues 9, 12, 16 and 20. This observation raises the question of whether AdE-1's mechanism of interaction with its target is identical with that of other sea anemone toxins.

Supporting the residue analysis described above, phylogenetic analysis places AdE-1 on a separate branch of the tree, distinct from both type 1 and type 2 neurotoxins (Figure 5B).

Comparison of the primary sequences of AdE-1 to Av2 and ApB

Structure–function studies analysing the effects of modifying sea anemone Na^+ channel toxins have mainly focused on mutated ApB, a toxin from the sea anemone *A. xanthogrammica*, and on Av2, a toxin from the sea anemone *A. viridis*, both of which are type 1 neurotoxins. The primary structures of these two toxins and their physiological activities are well characterized [35,44].

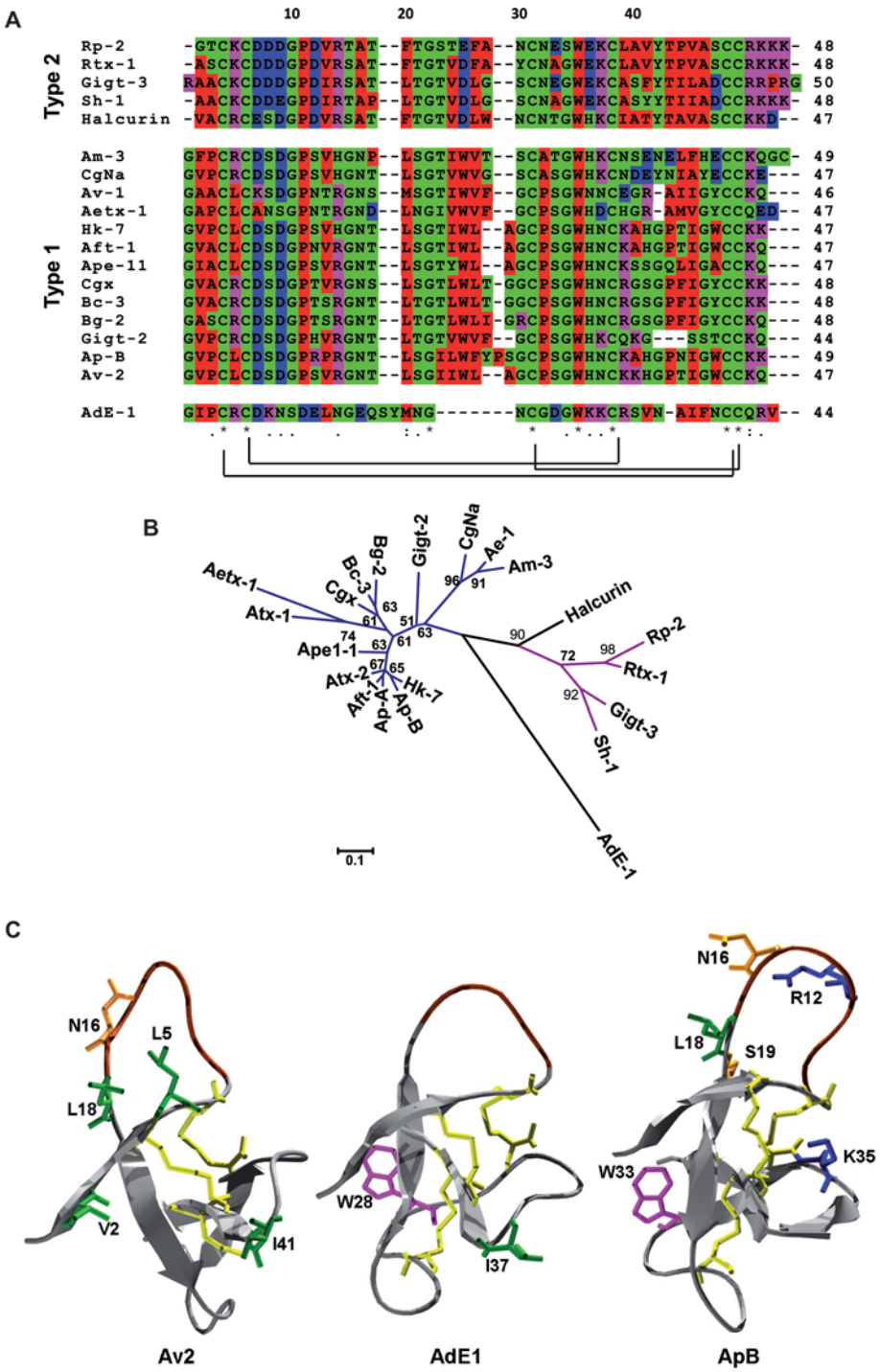

Figure 5 Comparison between AdE-1 and various sea anemone Na^+ channel type 1 and type 2 toxins

(**A**) Multiple sequence alignment of AdE-1 with various type 1 and 2 sea anemone Na^+ channel toxins. Lines indicate the probable disulfide bridge patterns which create the toxin scaffold. The colours are the ClustalW defaults: red represents small [small and hydrophobic (including aromatic tyrosine)], blue represents acidic, magenta represents basic, and green represents hydroxyl and amine and basic glutamine. *Identical residues in all sequences; :, conserved substitutions; and ., semi-conserved substitutions. (**B**) Evolutionary relationships of AdE-1 with type 1 and 2 sea anemone Na^+ channel toxins. The neighbor-joining tree emphasized the uniqueness of AdE-1 primary structure compared with other sea anemone type 1 and 2 Na^+ channel toxins. The tree shown is a bootstrap consensus tree inferred from 2000 replicates. The percentage of replicate trees in which the associated taxa clustered together in the bootstrap test is shown next to the branches. Branches corresponding to partitions reproduced in less than 50% bootstrap replicates were collapsed. The tree is drawn to scale and the evolutionary distances are given in the units of the number of amino acid substitutions per site. All positions containing gaps and missing data were eliminated. Type 2 toxin is in magenta and type 1 toxin in blue. Note that Halcurin may belong to either of the two groups. For the list of toxins from sea anemone species, refer to the Experimental section. (**C**) Comparison of the three-dimensional structural model of AdE-1 with Av2 and ApB. The three molecules are exhibited as silver ribbons. The Arg^{14} loop is indicated in bronze. The residues found to be involved in the activity of ApB and Av2 are presented as sticks. Residues with aliphatic side chains appear in green, aromatic in magenta, positively charged in blue and polar in orange. Disulfide bridges appear in yellow.

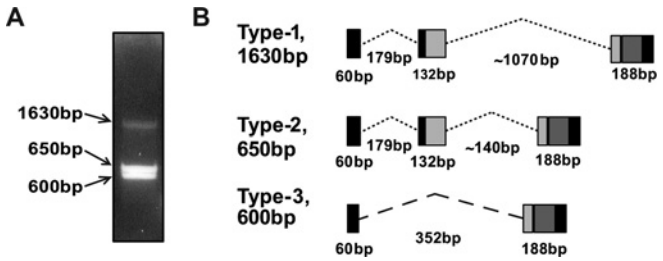

Figure 6 The three types of AdE-1-encoding DNA sequences

(**A**) Gel electrophoresis of the three types of AdE-1-encoding DNA sequences. These sequences were amplified from a genomic DNA batch which was extracted from three animals with specific primers designed from AdE-1 cDNA 5′-, and 3′-ends. (**B**) Schematic representation of the genomic organization of the three types of *AdE-1* gene. The introns are illustrated as dotted lines and the exons as filled boxes. The dashed line represents a region which differs significantly from the 1630 bp sequence. Dark grey boxes represent exon regions encoding the mature toxin, light grey boxes represent exon regions encoding the leader part and black boxes represent the exon region that encodes the 5′-and 3′-UTRs. The numbers beneath the diagram represent the sizes of the various segments.

In addition, the three-dimensional structure of ApB has been resolved by NMR (PDB code 1APF) [24]. Moran et al. [25] investigated the bioactive surface of Av2. A functional expression system was used to enable the mutation of the toxin residues and scan the mutant toxin's bioactivity. Their results revealed a functional role for Val^2, Leu^5, Asp^9, Asn^{16}, Leu^{20} and Ile^{45} and an additional functional role for Ser^{21} only on the cardiac channel subtype $hNa_V1.5$. Gly^{10} and Gly^{22} of Av2 appear to be important for toxin affinity to the channels. In addition, they suggest a pivotal role for Trp^{25} and Leu^{26} in folding and toxin structure.

ApB was expressed by Gallagher and Blumenthal [46] in *E. coli* cells to allow site-directed mutagenesis. Analysing the effects of the recombinant toxin and its mutants on neuronal and cardiac channel subtypes ($Na_V1.2$ and $Na_V1.5$ respectively) suggested a bioactive role for Arg^{12}, Pro^{13}, Asn^{16}, Leu^{20}, Ser^{21}, Trp^{35}, Lys^{39}, Trp^{47} and Lys^{51} [47–50]. Gly^{10} and Gly^{15} appear to be important for toxin affinity, and Gly^{22} is essential for folding determinant [43]. Comparison of the essential sites for activity in ApB and Av2 with the sequence of AdE-1 reveals great differences (Figure 5A). Except for Gly^{15}, Gly^{22} and Ile^{45}, all the essential residues in Av2 are substituted in AdE-1, and only three essential residues of ApB are not substituted (Gly^{15}, Gly^{22} and Trp^{35}). Of these substitutions, three in ApB and three in Av2 are chemically prominent: L5R, in which a hydrophobic amino acid is replaced by a basic one (in Av2); D9N, in which an acidic amino acid is replaced by a hydrophilic amino acid (in Av2); N16E, in which a hydrophilic amino acid is replaced by an acidic amino acid (in Av2 and in ApB); R12E, in which a basic amino acid is replaced by an acidic amino acid (in ApB) and W47N, in which a hydrophobic amino acid is replaced by a hydrophilic one (in ApB, Figure 5A). In addition, as mentioned above, the hydrophobic region between residues 23–27 which contains Trp^{25} and Leu^{26} (in Av2 and ApB) and is thought to play a pivotal role in folding and toxin structure, is completely absent in the sequence of AdE-1. This specific comprehension reveals the same conclusion of prominent differences in AdE-1 sequence and its uniqueness among other sea anemone toxins.

Comparison of the three-dimensional structural model of AdE-1 with Av2 and ApB

To further understand the differences in AdE-1 sequence, we constructed a three-dimensional model of the toxin, based on a model of the type 1 sea anemone toxin CgNa. The computational structural model of AdE-1 was aligned with the experimental model of ApB [24] and computational model of Av2 [25]. In addition to the differences in specific amino acids described above, the structural model suggests that the loop of AdE-1 is quite short and spans only residues 8–12, compared with residues 8–17 (Figure 5C) in ApB and Av2. Moreover, the lack of glycine residues indicates it has no flexibility like in other type 1 and type 2 sea anemone toxins. Since type 1 and type 2 sea anemone toxins exhibit sequence diversity, it was suggested that the common flexibility of the Arg^{14} loop has a pivotal role for their ability to bind Na^+ channels [9]. However, AdE-1 demonstrates that even this structural entity is not an absolute requirement, raising questions regarding the extent of the universality of structure–function in sea anemone toxins affecting Na^+ channels.

AUTHOR CONTRIBUTION

Nir Nesher performed most of the experiments, the analysis and wrote the paper; Eli Shapira contributed to the molecular biology; Daniel Sher contributed to sequence alignment and comprehension and writing; Yehu Moran contributed to the construction of the three-dimensional models and their interpretation; Liora Tsveyer contributed to Na^+ current experiments; Ana Luiza Turchetti-Maia contributed to writing the paper and Figure construction; Michal Horowitz and Binyamin Hochner were associated advisers; and Eliahu Zlotkin was the main adviser.

ACKNOWLEDGEMENTS

We thank Professor Philip Palade who provided the cardiomyocyte isolation protocol and the Charles E. Smith Family Laboratory for Collaborative Research in Psychobiology at The Hebrew University of Jerusalem (Jerusalem, Israel) for the use of their facilities.

FUNDING

This work was supported by the Israel Science Foundation [grant numbers 476/01 and 750/04]. A.L.T.M. is the recipient of a Golda Meir postdoctoral fellowship.

REFERENCES

1 Rothermel, B. A. and Hill, J. A. (2008) Autophagy in load-induced heart disease. Circ. Res. **103**, 1363–1369
2 Roger, V. L., Go, A. S., Lloyd-Jones, D. M., Benjamin, E. J., Berry, J. D., Borden, W. B., Bravata, D. M., Dai, S., Ford, E. S., Fox, C. S. et al. (2012) Heart disease and stroke statistics: 2012 update: a report from the American Heart Association. Circulation **125**, e2–e220
3 Hunt, S. A., Abraham, W. T., Chin, M. H., Feldman, A. M., Francis, G. S., Ganiats, T. G., Jessup, M., Konstam, M. A., Mancini, D. M., Michl, K. et al. (2009) 2009 focused update incorporated into the ACC/AHA 2005 Guidelines for the Diagnosis and Management of Heart Failure in Adults: a report of the American College of Cardiology Foundation/American Heart Association Task Force on Practice Guidelines: developed in collaboration with the International Society for Heart and Lung Transplantation. Circulation **119**, e391–e479
4 Landmesser, U. and Drexler, H. (2007) Update on inotropic therapy in the management of acute heart failure. Curr. Treat. Options Cardiovasc. Med. **9**, 443–449
5 DiBianco, R. (2003) Update on therapy for heart failure. Am. J. Med. **115**, 480–488
6 Norton, R. S. (2009) Structures of sea anemone toxins. Toxicon **54**, 1075–1088
7 Anderluh, G. and Macek, P. (2002) Cytolytic peptide and protein toxins from sea anemones (Anthozoa: Actiniaria). Toxicon **40**, 111–124
8 Honma, T. and Shiomi, K. (2006) Peptide toxins in sea anemones: structural and functional aspects. Mar. Biotechnol. (NY) **8**, 1–10
9 Smith, J. J. and Blumenthal, K. M. (2007) Site-3 sea anemone toxins: molecular probes of gating mechanisms in voltage-dependent sodium channels. Toxicon **49**, 159–170
10 Andreev, Y. A., Kozlov, S. A., Koshelev, S. G., Ivanova, E. A., Monastyrnaya, M. M., Kozlovskaya, E. P. and Grishin, E. V. (2008) Analgesic compound from sea anemone *Heteractis crispa* is the first polypeptide inhibitor of vanilloid receptor 1 (TRPV1). J. Biol. Chem. **283**, 23914–23921

11 Diochot, S., Salinas, M., Baron, A., Escoubas, P. and Lazdunski, M. (2007) Peptides inhibitors of acid-sensing ion channels. Toxicon **49**, 271–284
12 Sokotun, I. N., Il'ina, A. P., Monastyrnaya, M. M., Leychenko, E. V., Es'kov, A. A., Anastuk, S. D. and Kozlovskaya, E. P. (2007) Proteinase inhibitors from the tropical sea anemone *Radianthus macrodactylus*: isolation and characteristic. Biochemistry **72**, 301–306
13 Shiomi, K., Honma, T., Ide, M., Nagashima, Y., Ishida, M. and Chino, M. (2003) An epidermal growth factor-like toxin and two sodium channel toxins from the sea anemone *Stichodactyla gigantea*. Toxicon **41**, 229–236
14 Shibata, S., Norton, T. R., Izumi, T., Matsuo, T. and Katsuki, S. (1976) A polypeptide (AP-A) from sea anemone (*Anthopleura xanthogrammica*) with potent positive inotropic action. J. Pharmacol. Exp. Ther. **199**, 298–309
15 Schlesinger, A., Zlotkin, E., Kramarsky-Winter, E. and Loya, Y. (2009) Cnidarian internal stinging mechanism. Proc. Biol. Sci. **276**, 1063–1067
16 Myers, E. W. and Miller, W. (1988) Optimal alignments in linear space. Comput. Appl. Biosci. **4**, 11–17
17 Gasteiger E., Hoogland, C., Gattiker, A., Duvaud, S., Wilkins, M. R., Appel, R. D. and Bairoch, A. (2005) Protein identification and analysis tools on the ExPASy server. In The Proteomics Protocols Handbook (Walker, J. M., ed.), pp. 571–607, Humana Press, Totowa
18 Goujon, M., McWilliam, H., Li, W., Valentin, F., Squizzato, S., Paern, J. and Lopez, R. (2010) A new bioinformatics analysis tools framework at EMBL-EBI. Nucleic Acids Res. **38**, W695–W699
19 Larkin, M. A., Blackshields, G., Brown, N. P., Chenna, R., McGettigan, P. A., McWilliam, H., Valentin, F., Wallace, I. M., Wilm, A., Lopez, R. et al. (2007) ClustalW and ClustalX version 2. Bioinformatics **23**, 2947–2948
20 Tamura, K., Dudley, J., Nei, M. and Kumar, S. (2007) MEGA4: Molecular Evolutionary Genetics Analysis (MEGA) software version 4.0. Mol. Biol. Evol. **24**, 1596–1599
21 Saitou, N. and Nei, M. (1987) The neighbor-joining method: a new method for reconstructing phylogenetic trees. Mol. Biol. Evol. **4**, 406–425
22 Felsenstein, J. (1985) Confidence limits on phylogenies: an approach using the bootstrap. Evolution **39**, 783–791
23 Schwede, T., Kopp, J., Guex, N. and Peitsch, M. C. (2003) SWISS-MODEL: an automated protein homology-modeling server. Nucleic Acids Res. **31**, 3381–3385
24 Monks, S. A., Pallaghy, P. K., Scanlon, M. J. and Norton, R. S. (1995) Solution structure of the cardiostimulant polypeptide anthopleurin-B and comparison with anthopleurin-A. Structure **3**, 791–803
25 Moran, Y., Cohen, L., Kahn, R., Karbat, I., Gordon, D. and Gurevitz, M. (2006) Expression and mutagenesis of the sea anemone toxin Av2 reveals key amino acid residues important for activity on voltage-gated sodium channels. Biochemistry **45**, 8864–8873
26 Primor, N. and Zlotkin, E. (1975) On the ichthyotoxic and hemolytic action of the skin secretion of the flatfish *Pardachirus marmoratus* (Soleidae). Toxicon **13**, 227–231
27 Zlotkin, E., Fraenkel, G., Miranda, F. and Lissitzky, S. (1971) The effect of scorpion venom on blowfly larvae: a new method for the evaluation of scorpion venoms potency. Toxicon **9**, 1–8
28 Ravens, U., Davia, K., Davies, C. H., O'Gara, P., Drake-Holland, A. J., Hynd, J. W., Noble, M. I. and Harding, S. E. (1996) Tachycardia-induced failure alters contractile properties of canine ventricular myocytes. Cardiovasc. Res. **32**, 613–621
29 Dascal, N., Landau, E. M. and Lass, Y. (1984) *Xenopus* oocyte resting potential, muscarinic responses and the role of calcium and guanosine 3′,5′-cyclic monophosphate. J. Physiol. **352**, 551–574
30 Dascal, N., Snutch, T. P., Lübbert, H., Davidson, N. and Lester, H. A. (1986) Expression and modulation of voltage-gated calcium channels after RNA injection in *Xenopus* oocytes. Science **7**, 1147–1150
31 Beress, L. and Beress, R. (1975) Purification of three polypeptides with neuro- and cardiotoxic activity from the sea anemone *Anemonia sulcata*. Toxicon **13**, 359–367
32 Bers, D. M. (2002) Cardiac excitation–contraction coupling. Nature **415**, 198–205
33 Roden, D. M., Balser, J. R., George, Jr, A. L. and Anderson, M. E. (2002) Cardiac ion channels. Annu. Rev. Physiol. **64**, 431–475
34 Romey, G., Renaud, J. F., Fosset, M. and Lazdunski, M. (1980) Pharmacological properties of the interaction of a sea anemone polypeptide toxin with cardiac cells in culture. J. Pharmacol. Exp. Ther. **213**, 607–615
35 Isenberg, G. and Ravens, U. (1984) The effects of the *Anemonia sulcata* toxin (ATX II) on membrane currents of isolated mammalian myocytes. J. Physiol. **357**, 127–149
36 Song, Y., Shryock, J. C. and Belardinelli, L. (2008) An increase of late sodium current induces delayed afterdepolarizations and sustained triggered activity in atrial myocytes. Am. J. Physiol. Heart Circ. Physiol. **294**, H2031–H2039
37 Anderluh, G., Podlesek, Z. and Macek, P. (2000) A common motif in proparts of Cnidarian toxins and nematocyst collagens and its putative role. Biochim. Biophys. Acta **1476**, 372–376
38 Tekook, M. A., Fabritz, L., Kirchhof, P., Konig, S., Muller, F. U., Schmitz, W., Tal, T., Zlotkin, E. and Kirchhefer, U. (2012) Gene construction, expression and functional testing of an inotropic peptide from the venom of the black scorpion *Hottentotta judaicus*. Toxicon **60**, 1415–1427
39 Schiavon, E., Stevens, M., Zaharenko, A. J., Konno, K., Tytgat, J. and Wanke, E. (2010) Voltage-gated sodium channel isoform-specific effects of pompilidotoxins. FEBS J. **277**, 918–930
40 Moran, Y., Gordon, D. and Gurevitz, M. (2009) Sea anemone toxins affecting voltage-gated sodium channels: molecular and evolutionary features. Toxicon **54**, 1089–1101
41 Moran, Y., Weinberger, H., Sullivan, J. C., Reitzel, A. M., Finnerty, J. R. and Gurevitz, M. (2008) Concerted evolution of sea anemone neurotoxin genes is revealed through analysis of the *Nematostella vectensis* genome. Mol. Biol. Evol. **25**, 737–747
42 Honma, T., Hasegawa, Y., Ishida, M., Nagai, H., Nagashima, Y. and Shiomi, K. (2005) Isolation and molecular cloning of novel peptide toxins from the sea anemone *Antheopsis maculata*. Toxicon **45**, 33–41
43 Seibert, A. L., Liu, J., Hanck, D. A. and Blumenthal, K. M. (2003) Arg^{14} loop of site 3 anemone toxins: effects of glycine replacement on toxin affinity. Biochemistry **42**, 14515–14521
44 Bosmans, F. and Tytgat, J. (2007) Sea anemone venom as a source of insecticidal peptides acting on voltage-gated Na^+ channels. Toxicon **49**, 550–560
45 Wanke, E., Zaharenko, A. J., Redaelli, E. and Schiavon, E. (2009) Actions of sea anemone type 1 neurotoxins on voltage-gated sodium channel isoforms. Toxicon **54**, 1102–1111
46 Gallagher, M. J. and Blumenthal, K. M. (1992) Cloning and expression of wild-type and mutant forms of the cardiotonic polypeptide anthopleurin B. J. Biol. Chem. **267**, 13958–13963
47 Dias-Kadambi, B. L., Combs, K. A., Drum, C. L., Hanck, D. A. and Blumenthal, K. M. (1996) The role of exposed tryptophan residues in the activity of the cardiotonic polypeptide anthopleurin B. J. Biol. Chem. **271**, 23828–23835
48 Khera, P. K. and Blumenthal, K. M. (1996) Importance of highly conserved anionic residues and electrostatic interactions in the activity and structure of the cardiotonic polypeptide anthopleurin B. Biochemistry **35**, 3503–3507
49 Kelso, G. J., Drum, C. L., Hanck, D. A. and Blumenthal, K. M. (1996) Role for Pro^{13} in directing high-affinity binding of anthopleurin B to the voltage-sensitive sodium channel. Biochemistry **35**, 14157–14164
50 Seibert, A. L., Liu, J., Hanck, D. A. and Blumenthal, K. M. (2004) Role of Asn^{16} and Ser^{19} in anthopleurin B binding. Implications for the electrostatic nature of Na_V site 3. Biochemistry **43**, 7082–7089

Received 24 October 2012/14 January 2013; accepted 28 January 2013
Published as BJ Immediate Publication 28 January 2013, doi:10.1042/BJ20121623

Biochem. J. (2013) **451**, 81–90 (Printed in Great Britain) doi:10.1042/BJ20121623

online data

SUPPLEMENTARY ONLINE DATA

AdE-1, a new inotropic Na^+ channel toxin from *Aiptasia diaphana*, is similar to, yet distinct from, known anemone Na^+ channel toxins

Nir NESHER*†[1], Eli SHAPIRA†, Daniel SHER*‡, Yehu MORAN§, Liora TSVEYER‖, Ana Luiza TURCHETTI-MAIA¶**, Michal HOROWITZ††, Binyamin HOCHNER†** and Eliahu ZLOTKIN*[2]

*Department of Cell and Animal Biology, Institute of Life Sciences, The Hebrew University of Jerusalem, Jerusalem, Israel, †Smith Center for Psychobiology, Institute of Life Sciences, The Hebrew University of Jerusalem, Jerusalem, Israel, ‡Department of Marine Biology, Leon H. Charney School of Marine Sciences, University of Haifa, Haifa, Israel, §Department for Molecular Evolution and Development, Faculty of Life Sciences, University of Vienna, Vienna, Austria, ¶Alomone Labs, Jerusalem, Israel, ‖The Edmond and Lily Safra Center for Brain Sciences, The Hebrew University of Jerusalem, Jerusalem, Israel, **Department of Neurobiology, Institute of Life Sciences, The Hebrew University of Jerusalem, Jerusalem, Israel, and ††Laboratory of Environmental Physiology, Faculty of Dental Medicine, The Hebrew University of Jerusalem, Jerusalem, Israel

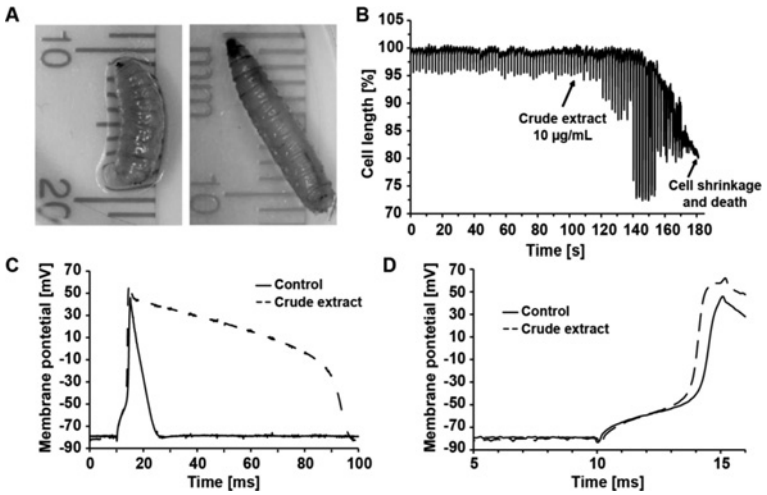

Figure S1 The physiological effects of *A. diaphana* crude extract

(**A**) Injection of about 1 μg of dry crude extract/g of body mass into *S. falculata* larvae resulted in immediate paralysis and body contraction (left-hand panel). The right-hand panel shows the control, injected with the same volume of DDW without the crude extract. (**B**) Crude extract (10 μg/ml) amplified cardiomyocyte contraction and initiated additional spontaneous and irregular contractions. (**C** and **D**) Injected at 50 μg/ml the crude extract prolonged the cardiomyocyte AP, increased its peak amplitude and steepened the phase 0 slope.

[1] To whom correspondence should be addressed (email nir.nesher@mail.huji.ac.il).
[2] This work is dedicated to the memory of Professor E. Zlotkin, a true scientist and a mentor.

```
1   CCA TTT GGA AGT TCT TCA AGA AAA AGA CAT TCG AAG AAA AGT CGG GAC TAA AAA CAG TTA
1               M   K   T   A   M   L   I   A   V   L   G   F   C   A   A   L   C
61  CTA AAA GCA ATG AAG ACT GCA ATG CTG ATC GCG GTT TTG GGC TTT TGT GCT GCC CTT TGT
18   F   V   E   S   S   H   E   E   E   R   E   A   A   V   Y   L   T   D   L   V
121 TTT GTC GAG AGC TCC CAT GAG GAA GAG AGG GAA GCC GCA GTT TAC TTG ACT GAT CTT GTC
38   S   K   A   E   S   A   I   K   R   G   I   P   C   R   C   D   K   N   S   D
181 TCG AAG GCA GAA AGT GCA ATC AAG CGT GGC ATT CCT TGC AGA TGC GAT AAG AAT TCA GAT
58   E   L   N   G   E   Q   S   Y   M   N   G   N   C   G   D   G   W   K   K   C
241 GAA CTA AAC GGA GAG CAG TCG TAC ATG AAT GGA AAC TGT GGT GAC GGT TGG AAA AAA TGC
78   R   S   V   N   A   I   F   N   C   C   Q   R   V   *   *
301 AGA AGT GTC AAT GCA ATT TTC AAT TGT TGT CAA AGA GTT TAG TAA TGC AAC AAT AAT AAT
361 AAA ATT ATT TAA AAA CTG AAA AAA AAA AAA
```

Figure S2 AdE-1 precursor, cDNA and amino acid sequences

Black residues, the 5′- and 3′-UTR; red residues, the pro-part, probably composed of a pro-peptide and a signal peptide; and blue residues, the mature peptide. Asterisks denote the stop codon. The parts of the sequence identified by the Edman degradation are underlined.

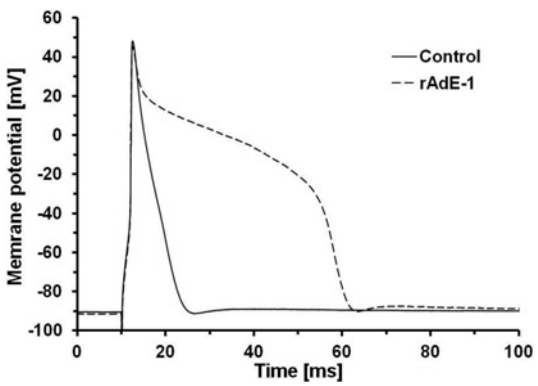

Figure S3 Recombinant AdE-1 mimics the effect of the natural peptide

rAdE-1 (100 ng/ml) prolonged the cardiomyocytes APD and slightly decreased its amplitude ($n = 3$). Note that 100 ng/ml of the rAdE-1 (molecular mass ~ 33 kDa) has almost the same molar concentration as 10 ng/ml of the purified AdE-1 (molecular mass ~ 5 kDa), ~ 3 nM and ~ 2 nM respectively. As a negative control we expressed, purified and assayed in the same manner, a toxin from wasps, β-PMTX (β-pompilidotoxin; GenPept accession number P69392) and a toxin from the scorpion (GenPept AAV54593), both known to affect neuronal Na^+ channels, but not the cardiac Na^+ channels subtype ($Na_V1.5$) and the cardiomyocyte AP. As expected, the two recombinant toxins resulting from this expression caused contraction and paralysis in blowfly larvae and had no effect on cardiomyocyte AP (results not shown), thus confirming that the effects observed with the AdE-1 were not owing to the mCherry, the His tag or to the buffers used in extraction and purification of the proteins, but due to the recombinant AdE-1 itself.

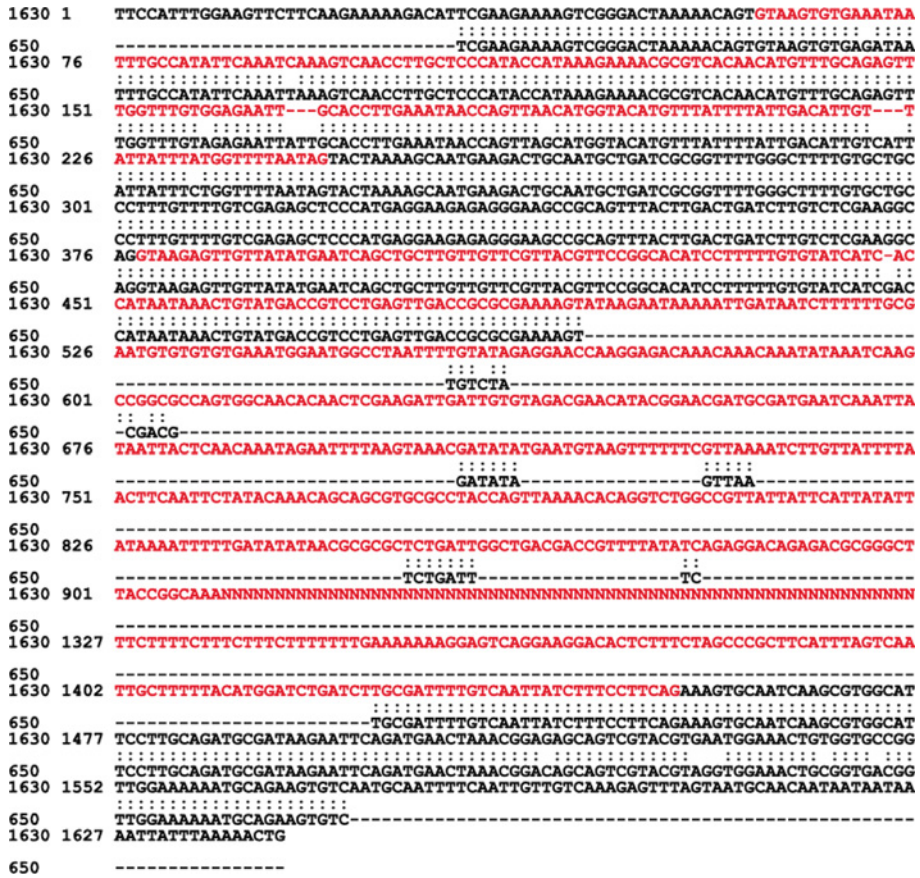

Figure S4 Global alignment of AdE-1 1630 bp and the 650 bp DNA gene sequences

Introns are coloured red, and exons are coloured black. N, a section with undefined bases.

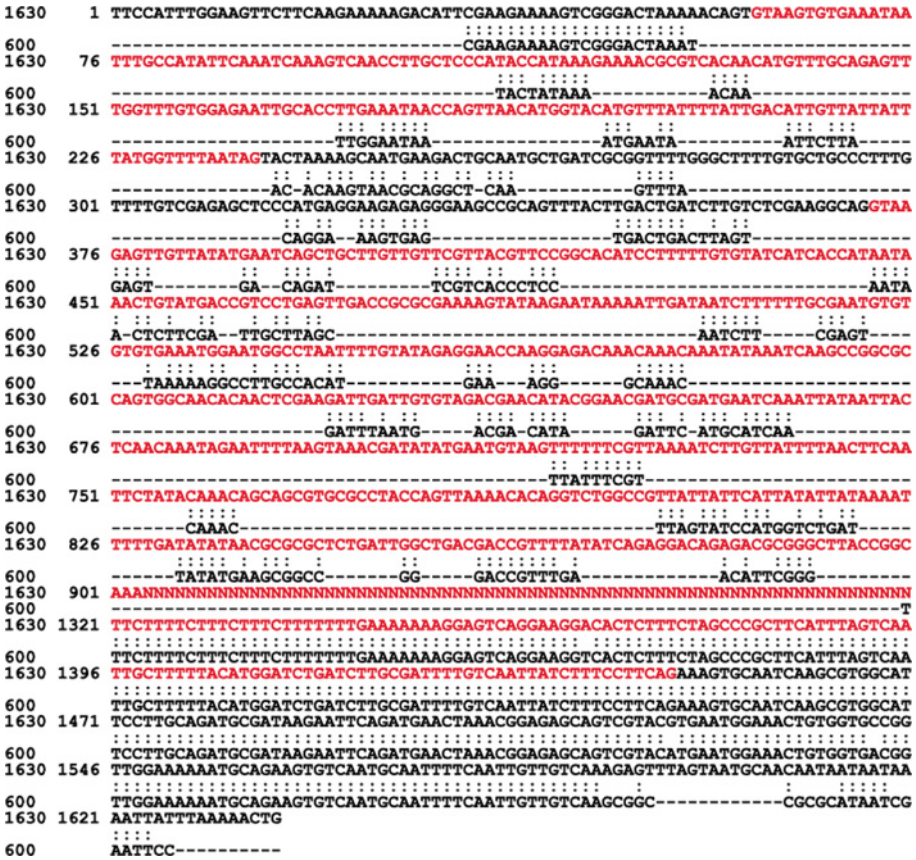

Figure S5 Global alignment of AdE-1 1630 bp and the 600 bp DNA gene sequences

Introns are coloured red, and exons are coloured black. N, a section with undefined bases.

Received 24 October 2012/14 January 2013; accepted 28 January 2013
Published as BJ Immediate Publication 28 January 2013, doi:10.1042/BJ20121623